Transcriptomic Analysis of *Streptococcus agalactiae* Periprosthetic Joint Infection

Hye-Kyung Cho,[1] Thao Masters,[1] Kerryl E. c,[1] Stephen Johnson,[2] Patricio R. Jeraldo,[3,4] Nicholas Chia,[3,4] Meng Pu,[5] Matthew P. Abdel, [6] Robin Patel[1,7]

[1]Division of Clinical Microbiology, Department of Laboratory Medicine and Pathology, Mayo Clinic, Rochester, MN

[2]Department of Health Sciences Research, Mayo Clinic, Rochester, MN

[3]Center for Individualized Medicine, Mayo Clinic, Rochester, MN

[4]Department of Surgery, Mayo Clinic, Rochester, MN

[5]Department of Medicine, Division of Gastroenterology and Hepatology, Mayo Clinic, Rochester, MN

[6]Department of Orthopedic Surgery, Mayo Clinic, Rochester, MN

[7]Division of Infectious Diseases, Department of Medicine, Mayo Clinic, Rochester, MN

Corresponding author: Robin Patel, M.D.

Division of Clinical Microbiology,

Mayo Clinic, Rochester, MN 55905

Phone: (507) 538-0579

email: patel.robin@mayo.edu

ABSTRACT

Although *Streptococcus agalactiae* periprosthetic joint infection (PJI) is not as prevalent as staphylococcal PJI, invasive *S. agalactiae* infection has recently increased in incidence. Here, RNA-Seq was used to perform transcriptomic analysis of *S. agalactiae* PJI using fluid derived from sonication of explanted arthroplasties of subjects with *S. agalactiae* PJI, with results compared to those of *S. agalactiae* strain NEM316 grown *in vitro*. 227 genes with outlier expression were found (164 up-regulated and 63 down-regulated) between PJI sonicate fluid and *in vitro* conditions. Functional enrichment analysis showed genes involved in mobilome and inorganic ion transport and metabolism to be most enriched. Genes involved in nickel, copper, and zinc transport, were upregulated. Among known virulence factors, *cyl* operon genes, encoding β-hemolysin/cytolysin, were consistently highly expressed in PJI *versus in vitro*. The data presented provide insight into *S. agalactiae* PJI pathogenesis and may be a useful resource for the identification of novel PJI therapeutics or vaccines against invasive *S. agalactiae* infections.

Keywords: *Streptococcus agalactiae*; prosthesis-related infections; RNA-seq; transcriptome

INTRODUCTION

Periprosthetic joint infection (PJI) causes significant morbidity and mortality, and healthcare cost burden (Bozic *et al.*, 2010, Bozic *et al.*, 2009, Brochin *et al.*, 2018, Kurtz *et al.*, 2012, Lum *et al.*, 2018, Natsuhara *et al.*, 2019). *Staphylococcus aureus* and *Staphylococcus epidermidis* are the most frequent causes of PJI, causing □65% of cases (Zimmerli *et al.*, 2004). However, other bacteria, including streptococci, enterococci, and Gram-negative bacilli, also contribute to PJI; conceivably, each could be considered as causing a distinct disease state.

Streptococcus agalactiae, a component of the gastrointestinal microbiota also found in the genitourinary tract of some adults, is an important pathogen in newborns and pregnant women. Recently, the incidence of invasive *S. agalactiae* infections has been increasing in non-pregnant adults, particularly among those with co-morbidities and older individuals (Edwards & Baker, 2005). While there is a difference in serotype distribution of *S. agalactiae* causing neonatal and adult diseases (Schuchat, 1998), other characteristics of the bacterium that might affect these two populations have not been elucidated.

Bone and joint infections, including osteomyelitis, spondylodiscitis, and native and periprosthetic joint infection, are common manifestations of *S. agalactiae* infections in adults (Oppegaard *et al.*, 2016, Corvec *et al.*, 2011, Farley & Strasbaugh, 2001). *S. agalactiae* is responsible for <10% of PJIs, most frequently causing “delayed” or “late-onset” PJI (Tande & Patel, 2014, Sendi *et al.*, 2011). Infection is presumed to be hematogenous in most cases, with the gastrointestinal tract, genitourinary tract, and possibly skin being common sources (Tande & Patel, 2014, Triesenberg *et al.*, 1992, Zeller *et al.*, 2009b). There are conflicting reports on the outcomes of *S. agalactiae* PJI. While some studies report remission rates of *S. agalactiae* PJI to be higher than those of staphylococcal PJI (Fiaux *et al.*, 2016), others suggest that streptococcal PJIs as a whole show high treatment failure rates (Akgün *et al.*,

2017), with *S. agalactiae* having worse outcomes than other *Streptococcus* species (Zeller *et al.*, 2009a, Mahieu *et al.*, 2019); reasons behind this are unknown.

Understanding transcript profiles of bacteria under physiological or pathological conditions may help identify genomic elements that contribute to disease processes (Wang *et al.*, 2009, Croucher & Thomson, 2010). Massive parallel sequencing can be used to analyze transcriptomes via complementary DNA (cDNA) sequencing – so-called, RNA-Seq (Kukurba & Montgomery, 2015, Wang *et al.*, 2009), providing all transcriptomic data in an unbiased manner and at a higher resolution than microarray or individual gene or gene panel analysis (Croucher & Thomson, 2010).

Here, a transcriptome study based on RNA-Seq analysis of *in vivo S. agalactiae* RNA from samples derived from sonication of explanted arthroplasties is presented. *S. agalactiae* PJI RNA-Seq data were compared to previously generated RNA-Seq data from *S. agalactiae* strain NEM316 grown *in vitro* (Rosinski-Chupin *et al.*, 2015), to explore PJI-specific gene expression profiles.

MATERIALS AND METHODS

Materials

Sonicate fluid samples collected between April 2005 and August 2016 from six patients who underwent hip or knee arthroplasty revision for *S. agalactiae* PJI were studied. A publicly available RNA Seq transcriptome dataset from *S. agalactiae* NEM316 [a serotype III (ST-23) reference strain from the blood of a neonate with early-onset *S. agalactiae* disease (Glaser *et al.*, 2002)] grown to mid-exponential phase in Todd Hewitt medium (three replicates), was used to compare gene expression patterns with RNA-Seq data from sonicate fluid samples (BioProject accession number PRJEB8097: https://www.ncbi.nlm.nih.gov/bioproject/PRJEB8097 [BioSample accessions SAMEA3180396, SAMEA3180402, SAMEA3180416]). The six *S. agalactiae* isolates cultured from sonicate fluid were also used for pan-genome construction.

Sample handling

Explanted prostheses were transported to the clinical microbiology laboratory in solid jars. Implant processing was performed according to an established clinical protocol that includes vortexing and sonication in Ringer's solution (Trampuz *et al.*, 2007). Sonicate fluid samples were immediately stored at -80°C without RNA an stabilizer until RNA was extracted and sequenced.

Bacterial whole genome sequencing and pan-genome construction

S. agalactiae was identified per standard protocols in the Mayo Clinic Clinical Microbiology Laboratory. *S. agalactiae* isolates were designated 1 to 6 corresponding to their associated subject number. Genomic DNA was extracted from the six isolates cultured from

PJI subjects using the Zymo Research Quick-DNA Fungal/Bacterial Miniprep kit (Zymo Research, Irvine, CA) and quantified using a Qubit 2.0 Fluorometer (Thermo Fisher Scientific, Coon Rapids, MN). Sequencing libraries were prepared using a Nextera® XT PE kit (Illumina, Inc., San Diego, CA). Sequencing was performed on an Illumina HiSeq 4000 with a 2X 150-base pair setting and 60 sample libraries multiplexed per flow cell.

Bacterial genomes were assembled from raw reads using a *de novo* assembler SKESA v2.4.0 (Souvorov *et al.*, 2018) and annotated by Prokka v1.14.5 using the *S. agalactiae* 2603V/R genome as the reference genome for purposes of gene annotation (Seemann, 2014). A pan-genome was constructed with Roary v3.13.0 using annotated fragmented *de novo* assemblies to identify core and accessory genes (Page *et al.*, 2015). This pan-genome served as a common reference for transcript quantification and outlier analysis between the RNA-Seq data from sonicate fluid and NEM316.

Phylogeny and virulence gene profiling

A phylogeny based on 1,000 common gene families across the 6 isolates plus *S. agalactiae* strains NEM316 and 2603V/R was constructed using the CodonTree method at the Phylogenetic Tree Building Service from PATRIC Bioinformatics Resource Center (Davis *et al.*, 2019). Phylogeny was midpoint rooted. Virulence gene content was profiled using the database of Virulence Factors of Pathogenic Bacteria (VFDB) (Liu *et al.*, 2019) through the interface at PATRIC.

Serotyping, multilocus sequence typing, and pilus island typing

Artemis was used to annotate and extract capsular locus sequences from *S. agalactiae* isolate whole genome sequences (Rutherford *et al.*, 2000). Extracted capsular

locus sequences from each isolate were used to assign serotype, based on the highest identity using a BLAST query. The sequence type (ST) of each *S. agalactiae* isolate was determined by comparing allelic profiles of housekeeping genes *adhP*, *pheS*, *atr*, *glnA*, *sdhA*, *glcK*, and *tkt* (Jones *et al.*, 2003) to the PubMLST *S. agalactiae* database (https://pubmlst.org/organisms/streptococcus-agalactiae) with SeqSphere+ software version 6.0.2 (Ridom GmbH, Münster, Germany). Pilus type was assigned by comparing allelic profiles of pilus genes (PI-1, *sag0645–0650*; PI-2a, *sag1404–1408*; PI-2b, *sag2190–2194*) with a sequence query to the database.

RNA isolation and sequencing

RNA from sonicate fluid was isolated using the miRNeasy Serum/Plasma kit (QIAGEN, Germantown, MD) and subjected to genomic DNA and bacterial ribosomal RNA (rRNA) removal using RNase-free DNase I (QIAGEN) and the Ribo-Zero rRNA removal kit (Bacteria) (Illumina, San Diego, CA). Following purification using an RNeasy MinElute Cleanup kit (QIAGEN), rRNA-depleted RNA was eluted in 30 µl RNAse-free water. RNA quantity and integrity were evaluated using a Qubit 2.0 Fluorometer coupled with a Qubit RNA high-sensitive assay kit (Thermo Fisher Scientific), and an Agilent 4200 TapeStation system (Agilent, Santa Clara, CA).

Next-generation sequencing cDNA libraries were constructed using the Ovation SoLo RNA-Seq System (NuGEN Technologies, San Carlos, CA) from 1 ng of input RNA, as previously described (Masters *et al.*, 2018). External RNA Control Consortium (ERCC) RNA Spike-In Mix 1 (Thermo Fisher Scientific, Waltham, MA) was used as a control to measure variability in the library generation process. Following cDNA synthesis and amplification, a SoLo AnyDeplete probe mix (NuGEN Technologies) was added to the libraries to deplete

human rRNA sequences. The resulting cDNA libraries were sequenced on an Illumina HiSeq 4000 with 10 samples multiplexed per lane, producing 100-base pair, paired-end reads.

RNA-Seq analysis

Raw sequencing reads were analyzed to identify microbial RNA, as previously described (Thoendel *et al.*, 2016), with minor modifications. RNA-Seq adapter sequences were trimmed with Atropos 1.1.19 (Didion *et al.*, 2017), and human reads removed using BioBloom tools 2.1.1 (Chu *et al.*, 2014). Taxonomy was assigned with Livermore Metagenomics Analysis Toolkit (LMAT) 1.2.6 using k-mer identifiers and the kML+H.noprune.4-14.2025.db database (Ames *et al.*, 2013).

RNA-Seq reads were pseudoaligned to the pan-genome constructed as described above (Tettelin *et al.*, 2005) and transcript abundances quantified using Kallisto version 0.42.4 (Bray *et al.*, 2016) and converted to transcripts per million (TPM). For the external NEM316 data, data from the three replicates were aggregated by calculating the mean TPM. Outlier expression analysis was performed by calculating a modified *z*-score for each gene g_{ij} in a sample *I* with *j* genes present in the core genome such that: $z = [\log_2(g_{ij}) - \text{median}(\log_2(g_i)] / [1.4826 * \text{MAD}(\log_2(g_i)]$, with a pseudocount added, if necessary. For this study, any gene with $|z| > 3$ was considered an outlier.

Homology modeling of protein structure

To predict protein homology, protein structures of selected genes were generated from amino acid sequences derived from RNA-Seq data using a web-based bioinformatics server, Phyre2 (Kelley *et al.*, 2015). Predicted structural models were retrieved for selected sequences, queried and templated in Phyre2, with a representation of structures drawn using

Chimera (Pettersen *et al.*, 2004).

Statistical analysis

Graphpad Prism (ver. 8.0, GraphPad Software San Diego, CA) was used for Fisher's exact test to access functional enrichment of differentially expressed genes belonging to the specific COG category.

RESULTS

Description of subjects

Six subjects with *S. agalactiae* PJI (mean age 62 years, range: 42–73 years) who underwent surgery at Mayo Clinic from 2006 to 2016 were studied, four (67%) of whom were male. All had local pain at the involved site, with fevers and/or chills. Two had undergone hip and four knee arthroplasty. The age of implanted material at the time of surgery ranged from 29 days to 5.4 years, including 2 cases of "early" (less than 3 months after placement), 1 of "delayed" (3 months to 1–2 years after placement) and 3 of "late" (more than 1–2 years after implantation) infection (Tande & Patel, 2014). *S. agalactiae* was isolated from sonicate fluid culture from all subjects (Table 1). There was no obvious co-infection.

Genomic description of S. agalactiae isolates

Whole-genome sequencing of the cultured isolates showed the isolates to have diverse characteristics. Three isolates displayed serotype V, two serotype Ia, and one serotype

II (Table 1). There was also diversity in isolate multi-locus sequence types (Table 1), with one isolate (IDRL-7656/subject 2) displaying a novel sequence type due to a novel allele for *adhP* in the region used for typing. A phylogenetic analysis of the isolates, which included NEM316 (serotype III) and 2603V/R (serotype V) as references, recapitulated the diversity findings, with the serotype V isolates clustering together, and other isolates showing differences from one another (Figure A1 in Appendix). When screening for virulence genes against the Virulence Factors in Pathogenic Bacteria (VFDB) database (Liu *et al.*, 2019), while the isolates had similar complements of virulence genes, they exhibited expected variation in the architecture of the capsular polysaccharide genes corresponding to their respective serotypes. Fibrinogen-binding surface protein genes *fbsA and fbsB* were found in IDRL-7656 and IDRL-8557. While the presence of pilus-associated genes showed slight differences between the isolates, all genes belonging to *cyl* operon were detected in all isolates (Table S1: https://doi.org/10.5281/zenodo.5717630).

S. agalactiae expression profiles by outlier expression analysis

Total read counts of transcripts from sonicate fluids ranged from 31,291 to 522,023. Since samples 1 and 4 had low read counts of non-rRNA transcripts, they were excluded from expression analysis studies (Table A1 in Appendix). Read counts of non-rRNA transcripts from *S. agalactiae* strain NEM316 RNA-Seq are shown in Table A2. The *S. agalactiae* pan-genome constructed from the associated PJI isolates, comprised of 2,738 genes, of which 1,683 were identified as core genes, was used to quantify bacterial transcripts from PJI and the *in vitro* NEM316 strain. There were 227 genes identified as strong outliers (*in vitro* $|z| > 3$, where z is a modified z score—see Methods) in expression between PJI (*in vivo*) and *in vitro* conditions. Of these, 164 were up-regulated (*in vitro* $z < -3$), and 63 down-regulated (*in vitro* $z > 3$) in sonicate fluid compared to *in vitro*. Genes with detected outlier

expression are listed in Table S2 (https://doi.org/10.5281/zenodo.5717630) and whole core gene lists are shown in Table S3 (https://doi.org/10.5281/zenodo.5717630), identified by the matching locus tag in *S. agalactiae* 2603V/R used as an annotation reference.

nik operon genes (*sag1514-1518*), *cop* operon genes (*sag0384-0386*), and *lmb-phtD* operon genes (*sag1233-1234*), encoding known or predicted metal transport systems, were highly expressed in sonicate fluid. *sag1514-1518* comprise an operon putatively involved in the intake of nickel/cobalt via *nikA–E* (ABC transporter), which are homologous with genes involved in a nickel/cobalt uptake system in *S. aureus*, *cntA-D,* and *cntF,* which has been shown to contribute to *S. aureus* virulence (Remy *et al.*, 2013). The function of these genes in *S. agalactiae* disease has not, however, been demonstrated. The predicted structure of the SAG1518 protein is homologous to the structure of NikA from *Brucella suis* (protein data bank [PDB] ID: 4OER), with 93% coverage and 41% identity based on Phyre2 prediction (Kelley *et al.*, 2015) and Chimera (Pettersen *et al.*, 2004) alignment of the two structures (Table A3, Figure A2 in Appendix).

sag0384-0386 (*copR, copA,* and *copZ*) belonging to *cop* operon were highly expressed in sonicate fluid *versus in vitro* (z = -5.152, -16.313, and -1.386, respectively). *sag1264* encoding transcriptional repressor CopY was not detected in the *in vitro* strain.

sag1234 encoding laminin-binding protein (Lmb) and *sag1233* encoding streptococcal histidine triad family protein (PhtD or Sht), were highly expressed in sonicate fluid. The Lmb protein of *S. agalactiae*, also known as an adhesin that binds a human extracellular matrix component called laminin, has been shown to involve in zinc uptake (Moulin *et al.*, 2016). Two Lmb homologs, AdcA (SAG0535) and AdcAII (SAG1938), redundant binding proteins that combine with the AdcCB translocon (SAG0155 and SAG0156) form a zinc-ABC transporter, with their expression controlled by zinc-dependent regulator AdcR (SAG0154) (Moulin *et al.*, 2016). In this study, the expression of *sag0535*

and *sag0154-0156* was highly expressed in sonicate fluid compared to the *in vitro* strain, and *sag1938* was not detected in the *in vitro* strain.

Functional enrichment

Functional enrichment analysis of outlier genes revealed genes involved in mobilome and those in inorganic ion transport and metabolism to be most enriched in sonicate fluid (Figure 2). The most interesting genes in the outlier analysis, *nik, lmb-phtD,* and *cop* operons, belonged to the inorganic ion transport and metabolism functional category. The pathogenic roles of the genes belonging to the mobilome are unknown.

Genes labeled as being involved in energy production and conversion based on Database of Clusters of Orthologous Genes (COGs) (https://www.ncbi.nlm.nih.gov/research/cog) showed decreased expression in PJI *versus in vitro*, with the most down-regulated genes in this category encoding F0F1 ATP synthase subunit C, alpha, gamma, and epsilon (*sag0857*, *sag0861*, *sag0862*, and *sag0864*, respectively).

Genes associated with *S. agalactiae* adhesion and biofilm formation

Adhesion factors, pilus islands (PI), and sortases

Expression of genes encoding adhesion factors important in *S. agalactiae* biofilm formation was analyzed (Table S4: https://doi.org/10.5281/zenodo.5717630); *lmb* and *cspA* were up-regulated outliers, and *gap* down-regulated in sonicate fluid compared to *in vitro* (Figure 2A). All isolates that caused PJI had PI-2a, and four (including three of four isolates

subjected to outlier expression analysis) had PI-1, with *sag1408* encoding PI-2a a down-regulated outlier in sonicate fluid compared to *in vitro*. The gene encoding sortase, involved in cell wall anchoring of pilus polymers (Nobbs *et al.*, 2008) - *srtA* (*sag0961*) – was weakly more expressed in sonicate fluid compared to *in vitro* (Table S4: https://doi.org/10.5281/zenodo.5717630, Figure 2A).

Other virulence factors

cylA, B, D, E, F, G, I, J, K, X, Z, and *acpC*, encoding β-hemolysin/cytolysin were all up-regulated in sonicate fluid compared to *in vitro* (Figure 2B). Among genes involved in immune evasion, *neuC-D, cpsB, D, E,* and *cpsK* were down-regulated in sonicate fluid compared to *in vitro* (Table S4: https://doi.org/10.5281/zenodo.5717630, Figure 2B).

DISCUSSION

S. agalactiae is a leading pathogen of invasive disease in neonates and pregnant women and also in non-pregnant adults, especially those of older age or with underlying conditions. Since *S. agalactiae* infections in newborns and pregnant women are known to start from bacterial colonization of the vaginal tract, adhesion factors and other virulence factors associated with biofilm formation on the vaginal mucosa have been studied as contributors to colonization (Cook *et al.*, 2018, Sheen *et al.*, 2011). PJI is initiated through the introduction of microorganisms at surgery, the spread of infection from adjacent sites, or hematogenous seeding (Tande & Patel, 2014). Since bacteremia accompanies *S. agalactiae* PJI in up to 50% of cases, the hematogenous spread is thought to be an important source (Everts *et al.*, 2004). To establish infection, bacteria theoretically first colonize the gastrointestinal tract, genitourinary tract, and/or skin, where they form biofilms, and then

spread hematogenously, adhere to prostheses, and again form biofilms on the prostheses. Studies on this complex pathological process are, however, limited.

In this study, the most enriched functional gene category in PJI sonicate fluid was the inorganic ion transport and metabolism category, of which genes involved in nickel, zinc, and copper transport were highly expressed. Metals play a role in the life processes of microorganisms, with organisms having developed processes for their uptake. Pathogenic bacteria encounter metal restriction when placed in the metal-poor environment of their host (Hammer & Skaar, 2012). 'Nutritional immunity' set up by hosts to prevent bacterial growth presumably extends to many, if not all 'essential' micronutrients, with mechanisms having been described for sequestering zinc, iron, and manganese (Grim *et al.*, 2017, Kehl-Fie & Skaar, 2010). The synovial space and surrounding tissues in which PJI occurs are limited spatially and in terms of nutrients (Jackson & Gu, 2009). The action of micrometallic molecules on surrounding human tissues, prostheses, and causative bacteria is an interesting topic; this study provides insight into this process. Although means of metal acquisition are well-known for iron, manganese, and zinc (Corbin *et al.*, 2008), others metals in trace amounts may be important under specific conditions (Remy *et al.*, 2013). Nickel is a cofactor of bacterial enzymes potentially involved in a myriad of cellular processes (Mulrooney & Hausinger, 2003). For *Helicobacter pylori*, for example, nickel, a cofactor of urease, is essential for survival and successful colonization of human gastric mucosa (Molnar *et al.*, 2010). Recently, a nickel/cobalt uptake system (CntA–D and F/NikA–E) in *S. aureus* has been shown to contribute to the virulence of this species (Remy *et al.*, 2013). In a murine bacteremia model, mortality was lower in *S. aureus cnt* mutant infection compared to wild-type strain infection. Bladder and kidney colonization in a urinary tract infection model were reduced with the *cnt* mutant *versus* the wild-type strain (Remy *et al.*, 2013). In this study, *sag1514–1518* (*nikA–E*), genes putatively involved in nickel uptake, were highly expressed

in sonicate fluid. Although the roles of these genes have not been demonstrated in *S. agalactiae*, gene orthology suggests that they would function similarly to the *S. aureus* CntA-D and F system and play a role in PJI pathogenesis. The findings in *S. agalactiae* are novel and reported here for the first time. In addition, a transcriptome study revealed that *cnt* genes were up-regulated in *S. aureus* PJI sonicate fluid compared to the corresponding isolates grown *in vitro* (Le Masters et al., 2021). This consistent finding, the up-regulation of *nik* and *cnt* genes shown in *S. aureus* and *S. agalactiae* PJI, respectively, suggests a potential role of nickel/cobalt uptake system in the pathogenesis of PJI.

Copper is an essential metal element in bacterial cells. However, excessive copper is hazardous to cells due to free-radical damage (Ladomersky & Petris, 2015). Keeping a balance of copper at human pathogen interfaces is needed for bacterial survival and pathogenesis. *copA* encoding the copper-transporter ATPase CopA mediates the control of copper efflux in several human pathogens (White *et al.*, 2009, Macomber & Imlay, 2009, Ladomersky *et al.*, 2017, Johnson *et al.*, 2015). A recent study showed the role of this mechanism on the survival, growth, and virulence of *S. agalactiae* in the mammalian host (Sullivan *et al.*, 2021). Although copper levels in sonicate fluid were not determined in this study, it is known that copper is elevated in inflamed tissue (Djoko *et al.*, 2015). As copper levels in infected tissues increased, the expression of *cop* operon genes, which regulate copper efflux for virulence and survival of bacteria, may have increased in sonicate fluid.

Among the virulence factors studied, *lmb* and *csp*A were highly expressed in PJI compared to *in vitro*. Lmb is an adhesin that binds to laminin present in human tissue; it also promotes bacterial invasion in human brain microvascular endothelial cells (Tenenbaum *et al.*, 2007, Spellerberg *et al.*, 1999). Lmb is also involved in zinc uptake showing strong homology with the zinc-binding protein AdcA of other streptococcal species (Linke *et al.*, 2009, Bayle *et al.*, 2011). Zinc is also a trace element functioning as a cofactor for a number

of essential prokaryotic enzymes and transcriptional regulators. Pathogenic bacteria must adapt zinc transport mechanisms to accommodate these differences to both avoid toxicity and meet their requirements for this metal. In a zinc-deficient environment, zinc acquisition in streptococci is mostly performed by an ATP-binding cassette (ABC) transporter, which is composed of one or several metal-binding proteins (AdcA, Lbp, or Lmb), an integral membrane component (AdcB), and an ATPase (AdcC) (Moulin *et al.*, 2016). In contrast, in the presence of adequate intracellular zinc concentrations, the AdcR repressor regulator inhibits the expression of *adcABC* and *lmb*. In this study, these zinc uptake genes, *adcABC,* and *lmb* were highly expressed in sonicate fluid compared to *in vitro*, suggesting a potential role of increased zinc uptake in the pathogenesis of *S. agalactiae* PJI.

Although biofilm formation by *S. agalactiae* may be associated with PI-2a pilus production (Rinaudo *et al.*, 2010), expression of PI-2a pilus genes was down-regulated in sonicate fluid compared to *in vitro* in this study. While some studies have suggested that non-pilus adhesion regulated by *covR* may be a contributor to bacterial adherence and biofilm formation (Park *et al.*, 2012), *covR* (*sag0416*) expression was only weakly higher in sonicate fluid compared to *in vitro* conditions in this study. This suggests that biofilms formed on arthroplasty surfaces might be affected by the expression of non-pilus rather than pilus adhesins, or other mechanisms.

β-hemolysin/cytolysin (β-HC, also CylE), is a surface-associated, pluripotent toxin crucial for *S. agalactiae* pathogenesis; it promotes *S. agalactiae* invasion of lung epithelial and endothelial cells and the blood-brain barrier (Rajagopal, 2009). Hemolytic activity is associated with *S. agalactiae* colonization and pathogenesis, with hemolysin-deficient *S. agalactiae* mutants being attenuated for virulence in a *S. agalactiae* arthritis murine model; while more joint inflammation and damage were observed in hyperhemolytic mutant-infected animals than in those infected with the parental strain, non-hemolytic mutant-infected mice

had mild and transient arthritis (Puliti *et al.*, 2000). The *cyl* operon (*cylX-K*) is necessary for the synthesis of granadaene, the ornithine rhamnolipid pigment in *S. agalactiae,* which is hemolytic and cytotoxic to human amniotic epithelial cells and innate immune cells (Forquin *et al.*, 2007, Gottschalk *et al.*, 2006, Rosa-Fraile *et al.*, 2014, Armistead *et al.*, 2020, Whidbey *et al.*, 2013). In this study, all 12 genes belonging to *cyl* operon were highly expressed in PJI compared to *in vitro*, suggesting they could contribute to the pathogenesis of PJI.

S. agalactiae is encapsulated by a sialic acid capsular polysaccharide (CPS). Since sialic acid is also present on glycans of eukaryotic cells, the host may not recognize *S. agalactiae* as nonself (Rajagopal, 2009). Accordingly, CPS prevents complement factor C3 deposition and phagocytosis of *S. agalactiae* (Rajagopal, 2009). The genes required for CPS synthesis are part of a single *cps* locus, harboring a variable serotype-determining region (*cpsG–cpsK*) flanked by other CPS genes (*cpsA–cpsF* and *neuB–neuA*) conserved among the different serotypes (Cieslewicz *et al.*, 2005). In this study, expression of *cpsB*, *D*, *E*, *G*, and *K*, *neuC,* and *D* was down-regulated in the PJI compared to *in vitro*, albeit not among outliers. Contrary to recent studies that reported that *cps* genes are conditionally essential for the survival of S. *agalactiae* in human blood, the role of *cps* genes in PJI might be less significant (Hooven *et al.*, 2017).

There are several limitations to this study. Ideally, *in vitro* transcriptomic analysis of each isolate under conditions corresponding to each sample *in vivo* would have been helpful to understand the pathogenic role of the gene. NEM316 and the conditions under which it was grown *in vitro* may not be representative of the whole *S. agalactiae* population or the PJI isolates studies. NEM316 is a human strain from invasive disease and biofilm-producing, which is also relevant to PJI. In this study, functional validation of novel genes identified was not performed. Finally, gene expression may have been affected at least in part during the processes used to recover *S. agalactiae* from the prostheses. The lack of an RNA stabilizer is

also a limitation.

In conclusion, the data generated provides a glimpse into the transcriptomic landscape of *S. agalactiae* in the environment around prosthetic joints. Using outlier expression and functional enrichment analysis, the *nik* operon was up-regulated in PJI, suggesting a role of nickel transport in PJI pathogenesis. Among known virulence factors, β-HC was consistently up-regulated in PJI. The findings presented contribute to a deeper understanding of *S. agalactiae* PJI pathogenesis and provide molecular targets for the identification of novel PJI therapeutics or future vaccines against invasive infections caused by *S. agalactiae*.

ACKNOWLEDGEMENTS

Research reported in this publication was supported by the National Institute of Arthritis and Musculoskeletal and Skin Diseases of the National Institutes of Health under award number R01AR056647. The content is solely the responsibility of the authors and does not necessarily represent the official views of the National Institutes of Health.

Data availability statement

All data generated or analyzed during this study are included in this published article (and its supplementary files). New sequence data from this study have been deposited into NCBI under project no. PRJNA687554: https://www.ncbi.nlm.nih.gov/bioproject/PRJNA687554 (BioSample accessions: SAMN17305169-SAMN17305174). Supplemental data (Tables S1-S4) have been deposited on Zenodo (https://doi.org/10.5281/zenodo.5717630)

Ethics statement

This study was performed under approval from Mayo Clinic Institutional Review Board (protocol No. 09-000808).

CONFLICT OF INTERESTS

Dr. Patel reports grants from ContraFect, TenNor Therapeutics Limited, Hylomorph, BioFire, and Shionogi. Dr. Patel is a consultant to Curetis, Specific Technologies, Next Gen Diagnostics, PathoQuest, Selux Diagnostics, 1928 Diagnostics, PhAST, Torus, Mammoth Biosciences, and Qvella; monies are paid to Mayo Clinic. Dr. Patel is also a consultant to Netflix. In addition, Dr. Patel has a patent on *Bordetella pertussis/parapertussis* PCR issued, a patent on a device/method for sonication with royalties paid by Samsung to Mayo Clinic, and a patent on an anti-biofilm substance issued. Dr. Patel receives an editor's stipend from the Infectious Diseases Society of America (IDSA), and honoraria from the National Board of Medical Examiners (NBME), the Infectious Diseases Board Review Course, and UpToDate Inc. All other authors declare no conflicts of interest.

AUTHOR CONTRIBUTIONS

Hye-Kyung Cho
Conceptualization-Lead, Formal analysis-Lead, Writing – original draft-Lead

Thao Masters
Investigation-Supporting, Writing – review & editing-Supporting

Kerryl Greenwood-Quaintance
Supervision-Lead, Writing – review & editing-Supporting

Stephen Johnson
Data curation-Supporting, Writing – review & editing-Supporting

Patricio Jeraldo

Data curation-Supporting, Writing – review & editing-Supporting

Nicholas Chia
Validation-Supporting, Writing – review & editing-Supporting

Meng Pu
Investigation-Supporting, Writing – review & editing-Supporting

Matthew P. Abdel
Validation-Supporting, Writing – review & editing-Supporting

Robin Patel
Conceptualization-Supporting, Writing – review & editing-Lead

.

REFERENCES

Akgün, D., Trampuz, A., Perka, C., and Renz, N. (2017) High failure rates in treatment of streptococcal periprosthetic joint infection: Results from a seven-year retrospective cohort study. *Bone Joint J* **99-b**: 653-659.

Ames, S.K., Hysom, D.A., Gardner, S.N., Lloyd, G.S., Gokhale, M.B., and Allen, J.E. (2013) Scalable metagenomic taxonomy classification using a reference genome database. *Bioinformatics* **29**: 2253-2260.

Armistead, B., Whidbey, C., Iyer, L.M., Herrero-Foncubierta, P., Quach, P., Haidour, A., Aravind, L., Cuerva, J.M., Jaspan, H.B., and Rajagopal, L. (2020) The *cyl* genes reveal the biosynthetic and evolutionary origins of the group B Streptococcus hemolytic lipid, granadaene. *Front Microbiol* **10**.

Bayle, L., Chimalapati, S., Schoehn, G., Brown, J., Vernet, T., and Durmort, C. (2011) Zinc uptake by *Streptococcus pneumoniae* depends on both AdcA and AdcAII and is essential for normal bacterial morphology and virulence. *Mol Microbiol* **82**: 904-916.

Bozic, K.J., Kurtz, S.M., Lau, E., Ong, K., Chiu, V., Vail, T.P., Rubash, H.E., and Berry, D.J. (2010) The epidemiology of revision total knee arthroplasty in the United States. *Clin Ortho Rel Res* **468**: 45-51.

Bozic, K.J., Kurtz, S.M., Lau, E., Ong, K., Vail, T.P., and Berry, D.J. (2009) The epidemiology of revision total hip arthroplasty in the United States. *J Bone Joint Surg (Am)* **91**: 128-133.

Bray, N.L., Pimentel, H., Melsted, P., and Pachter, L. (2016) Near-optimal probabilistic RNA-seq quantification. *Nat Biotechnol* **34**: 525-527.

Brochin, R.L., Phan, K., Poeran, J., Zubizarreta, N., Galatz, L.M., and Moucha, C.S. (2018) Trends in periprosthetic hip infection and associated costs: A population-based study assessing the impact of hospital factors using national data. *J Arthroplasty* **33**: S233-S238.

Chu, J., Sadeghi, S., Raymond, A., Jackman, S.D., Nip, K.M., Mar, R., Mohamadi, H., Butterfield, Y.S., Robertson, A.G., and Birol, I. (2014) BioBloom tools: Fast, accurate and memory-efficient host species sequence screening using bloom filters. *Bioinformatics* **30**: 3402-3404.

Cieslewicz, M.J., Chaffin, D., Glusman, G., Kasper, D., Madan, A., Rodrigues, S., Fahey, J., Wessels, M.R., and Rubens, C.E. (2005) Structural and genetic diversity of group B streptococcus capsular polysaccharides. *Infect Immun* **73**: 3096-3103.

Cook, L.C.C., Hu, H., Maienschein-Cline, M., and Federle, M.J. (2018) A vaginal tract signal detected by the group B streptococcus SaeRS system elicits transcriptomic changes and enhances murine colonization. *Infect Immun* **86**.

Corbin, B.D., Seeley, E.H., Raab, A., Feldmann, J., Miller, M.R., Torres, V.J., Anderson, K.L., Dattilo, B.M., Dunman, P.M., Gerads, R., Caprioli, R.M., Nacken, W., Chazin, W.J., and Skaar, E.P. (2008) Metal chelation and inhibition of bacterial growth in tissue abscesses. *Science* **319**: 962-965.

Corvec, S., Illiaquer, M., Touchais, S., Boutoille, D., van der Mee-Marquet, N., Quentin, R., Reynaud, A., Lepelletier, D., Bémer, P., Bone, and Joint Infection Study, G. (2011) Clinical features of group B Streptococcus prosthetic joint infections and molecular characterization of isolates. *J Clin Microbiol* **49**: 380-382.

Croucher, N.J., and Thomson, N.R. (2010) Studying bacterial transcriptomes using RNA-seq. *Curr Opin*

Microbiol **13**: 619-624.
Davis, J.J., Wattam, A.R., Aziz, R.K., Brettin, T., Butler, R., Butler, R.M., Chlenski, P., Conrad, N., Dickerman, A., Dietrich, E.M., Gabbard, J.L., Gerdes, S., Guard, A., Kenyon, R.W., Machi, D., Mao, C., Murphy-Olson, D., Nguyen, M., Nordberg, E.K., Olsen, G.J., Olson, R.D., Overbeek, J.C., Overbeek, R., Parrello, B., Pusch, G.D., Shukla, M., Thomas, C., VanOeffelen, M., Vonstein, V., Warren, A.S., Xia, F., Xie, D., Yoo, H., and Stevens, R. (2019) The PATRIC Bioinformatics Resource Center: expanding data and analysis capabilities. *Nucleic Acids Res*.
Didion, J.P., Martin, M., and Collins, F.S. (2017) Atropos: specific, sensitive, and speedy trimming of sequencing reads. *PeerJ* **5**: e3720.
Djoko, K.Y., Ong, C.-l.Y., Walker, M.J., and McEwan, A.G. (2015) The role of copper and zinc toxicity in innate immune defense against bacterial pathogens. *J Biol Chem* **290**: 18954-18961.
Edwards, M.S., and Baker, C.J. (2005) Group B streptococcal infections in elderly adults. *Clin Infect Dis* **41**: 839-847.
Everts, R.J., Chambers, S.T., Murdoch, D.R., Rothwell, A.G., and McKie, J. (2004) Successful antimicrobial therapy and implant retention for streptococcal infection of prosthetic joints. *ANZ J Surg* **74**: 210-214.
Farley, M.M., and Strasbaugh, L.J. (2001) Group B streptococcal disease in nonpregnant adults. *Clin Infect Dis* **33**: 556-561.
Fiaux, E., Titecat, M., Robineau, O., Lora-Tamayo, J., El Samad, Y., Etienne, M., Frebourg, N., Blondiaux, N., Brunschweiler, B., Dujardin, F., Beltrand, E., Loiez, C., Cattoir, V., Canarelli, J.P., Hulet, C., Valette, M., Nguyen, S., Caron, F., Migaud, H., and Senneville, E. (2016) Outcome of patients with streptococcal prosthetic joint infections with special reference to rifampicin combinations. *BMC Infect Dis* **16**: 568.
Forquin, M.P., Tazi, A., Rosa-Fraile, M., Poyart, C., Trieu-Cuot, P., and Dramsi, S. (2007) The putative glycosyltransferase-encoding gene *cylJ* and the group B Streptococcus (GBS)-specific gene *cylK* modulate hemolysin production and virulence of GBS. *Infect Immun* **75**: 2063-2066.
Glaser, P., Rusniok, C., Buchrieser, C., Chevalier, F., Frangeul, L., Msadek, T., Zouine, M., Couvé, E., Lalioui, L., Poyart, C., Trieu-Cuot, P., and Kunst, F. (2002) Genome sequence of *Streptococcus agalactiae*, a pathogen causing invasive neonatal disease. *Mol Microbiol* **45**: 1499-1513.
Gottschalk, B., Bröker, G., Kuhn, M., Aymanns, S., Gleich-Theurer, U., and Spellerberg, B. (2006) Transport of multidrug resistance substrates by the *Streptococcus agalactiae* hemolysin transporter. *J Bacteriol* **188**: 5984-5992.
Grim, K.P., San Francisco, B., Radin, J.N., Brazel, E.B., Kelliher, J.L., Párraga Solórzano, P.K., Kim, P.C., McDevitt, C.A., and Kehl-Fie, T.E. (2017) The metallophore staphylopine ENABLES *Staphylococcus aureus* to compete with the host for zinc and overcome nutritional immunity. *mBio* **8**.
Hammer, N.D., and Skaar, E.P. (2012) The impact of metal sequestration on *Staphylococcus aureus* metabolism. *Curr Opin Microbiol* **15**: 10-14.
Hooven, T.A., Catomeris, A.J., Bonakdar, M., Tallon, L.J., Santana-Cruz, I., Ott, S., Daugherty, S.C., Tettelin, H., and Ratner, A.J. (2017) The *Streptococcus agalactiae* stringent response enhances virulence and persistence in human blood. *Infect Immun* **86**: e00612-00617.
Jackson, A., and Gu, W. (2009) Transport properties of cartilaginous tissues. *Curr Rheumatol Rev* **5**: 40.
Johnson, M.D., Kehl-Fie, T.E., Klein, R., Kelly, J., Burnham, C., Mann, B., and Rosch, J.W. (2015) Role of copper efflux in pneumococcal pathogenesis and resistance to macrophage-mediated immune clearance. *Infect Immun* **83**: 1684-1694.
Jones, N., Bohnsack, J.F., Takahashi, S., Oliver, K.A., Chan, M.-S., Kunst, F., Glaser, P., Rusniok, C., Crook, D.W.M., Harding, R.M., Bisharat, N., and Spratt, B.G. (2003) Multilocus sequence typing system for group B streptococcus. *J Clin Microbiol* **41**: 2530-2536.
Kehl-Fie, T.E., and Skaar, E.P. (2010) Nutritional immunity beyond iron: a role for manganese and zinc. *Curr Opin Chem Biol* **14**: 218-224.
Kelley, L.A., Mezulis, S., Yates, C.M., Wass, M.N., and Sternberg, M.J.E. (2015) The Phyre2 web portal for protein modeling, prediction and analysis. *Nat Protoc* **10**: 845-858.
Kukurba, K.R., and Montgomery, S.B. (2015) RNA sequencing and analysis. *Cold Spring Harb Protoc* **2015**: 951-969.
Kurtz, S.M., Lau, E., Watson, H., Schmier, J.K., and Parvizi, J. (2012) Economic burden of periprosthetic joint infection in the United States. *J Arthroplasty* **27**: 61-65.e61.
Ladomersky, E., Khan, A., Shanbhag, V., Cavet, J.S., Chan, J., Weisman, G.A., and Petris, M.J. (2017) Host and pathogen copper-transporting P-type ATPases function antagonistically during Salmonella infection. *Infect Immun* **85**.
Ladomersky, E., and Petris, M.J. (2015) Copper tolerance and virulence in bacteria. *Metallomics* **7**: 957-964.
Le Masters, T., Johnson, S., Jeraldo, P.R., Greenwood-Quaintance, K.E., Cunningham, S.A., Abdel, M.P., Chia, N., and Patel, R. (2021) Comparative transcriptomic analysis of *Staphylococcus aureus* associated with periprosthetic joint infection under *in vivo* and *in vitro* conditions. *J Mol Diagn* **23**: 986-999.

Linke, C., Caradoc-Davies, T.T., Young, P.G., Proft, T., and Baker, E.N. (2009) The laminin-binding protein Lbp from *Streptococcus pyogenes* is a zinc receptor. *J Bacteriol* **191**: 5814-5823.

Liu, B., Zheng, D., Jin, Q., Chen, L., and Yang, J. (2019) VFDB 2019: a comparative pathogenomic platform with an interactive web interface. *Nucleic Acids Res* **47**: D687-D692.

Lum, Z.C., Natsuhara, K.M., Shelton, T.J., Giordani, M., Pereira, G.C., and Meehan, J.P. (2018) Mortality during total knee periprosthetic joint infection. *J Arthroplasty* **33**: 3783-3788.

Macomber, L., and Imlay, J.A. (2009) The iron-sulfur clusters of dehydratases are primary intracellular targets of copper toxicity. *Proc Natl Acad Sci U S A* **106**: 8344-8349.

Mahieu, R., Dubée, V., Seegers, V., Lemarié, C., Ansart, S., Bernard, L., Le Moal, G., Asseray, N., Arvieux, C., Ramanantsoa, C., Cormier, H., Legrand, E., and Abgueguen, P. (2019) The prognosis of streptococcal prosthetic bone and joint infections depends on surgical management-A multicenter retrospective study. *Int J Infect Dis* **85**: 175-181.

Masters, T.L., Hilker, C.A., Jeraldo, P.R., Bhagwate, A.V., Greenwood-Quaintance, K.E., Eckloff, B.W., Chia, N., Hanssen, A.D., Abdel, M.P., Yao, J.Z., Jen, J., and Patel, R. (2018) Comparative evaluation of cDNA library construction approaches for RNA-Seq analysis from low RNA-content human specimens. *J Microbiol Methods* **154**: 55-62.

Molnar, B., Galamb, O., Sipos, F., Leiszter, K., and Tulassay, Z. (2010) Molecular pathogenesis of *Helicobacter pylori* infection: the role of bacterial virulence factors. *Dig Dis* **28**: 604-608.

Moulin, P., Patron, K., Cano, C., Zorgani, M.A., Camiade, E., Borezée-Durant, E., Rosenau, A., Mereghetti, L., and Hiron, A. (2016) The Adc/Lmb system mediates zinc acquisition in *Streptococcus agalactiae* and contributes to bacterial growth and survival. *J Bacteriol* **198**: 3265-3277.

Mulrooney, S.B., and Hausinger, R.P. (2003) Nickel uptake and utilization by microorganisms. *FEMS Microbiol Rev* **27**: 239-261.

Natsuhara, K.M., Shelton, T.J., Meehan, J.P., and Lum, Z.C. (2019) Mortality during total hip periprosthetic joint infection. *J Arthroplasty* **34**: S337-S342.

Nobbs, A.H., Rosini, R., Rinaudo, C.D., Maione, D., Grandi, G., and Telford, J.L. (2008) Sortase A utilizes an ancillary protein anchor for efficient cell wall anchoring of pili in *Streptococcus agalactiae*. *Infect Immun* **76**: 3550-3560.

Oppegaard, O., Skrede, S., Mylvaganam, H., and Kittang, B.R. (2016) Temporal trends of β-haemolytic streptococcal osteoarticular infections in western Norway. *BMC Infect Dis* **16**: 535.

Page, A.J., Cummins, C.A., Hunt, M., Wong, V.K., Reuter, S., Holden, M.T.G., Fookes, M., Falush, D., Keane, J.A., and Parkhill, J. (2015) Roary: rapid large-scale prokaryote pan genome analysis. *Bioinformatics* **31**: 3691-3693.

Park, S.E., Jiang, S., and Wessels, M.R. (2012) CsrRS and environmental pH regulate group B streptococcus adherence to human epithelial cells and extracellular matrix. *Infect Immun* **80**: 3975-3984.

Pettersen, E.F., Goddard, T.D., Huang, C.C., Couch, G.S., Greenblatt, D.M., Meng, E.C., and Ferrin, T.E. (2004) UCSF Chimera--a visualization system for exploratory research and analysis. *J Comput Chem* **25**: 1605-1612.

Puliti, M., Nizet, V., von Hunolstein, C., Bistoni, F., Mosci, P., Orefici, G., and Tissi, L. (2000) Severity of group B streptococcal arthritis is correlated with beta-hemolysin expression. *J Infect Dis* **182**: 824-832.

Rajagopal, L. (2009) Understanding the regulation of group B streptococcal virulence factors. *Future Microbiol* **4**: 201-221.

Remy, L., Carrière, M., Derré-Bobillot, A., Martini, C., Sanguinetti, M., and Borezée-Durant, E. (2013) The *Staphylococcus aureus* Opp1 ABC transporter imports nickel and cobalt in zinc-depleted conditions and contributes to virulence. *Mol Microbiol* **87**: 730-743.

Rinaudo, C.D., Rosini, R., Galeotti, C.L., Berti, F., Necchi, F., Reguzzi, V., Ghezzo, C., Telford, J.L., Grandi, G., and Maione, D. (2010) Specific involvement of pilus type 2a in biofilm formation in group B Streptococcus. *PLoS One* **5**: e9216.

Rosa-Fraile, M., Dramsi, S., and Spellerberg, B. (2014) Group B streptococcal haemolysin and pigment, a tale of twins. *FEMS Microbiol Rev* **38**: 932-946.

Rosinski-Chupin, I., Sauvage, E., Sismeiro, O., Villain, A., Da Cunha, V., Caliot, M.E., Dillies, M.A., Trieu-Cuot, P., Bouloc, P., Lartigue, M.F., and Glaser, P. (2015) Single nucleotide resolution RNA-seq uncovers new regulatory mechanisms in the opportunistic pathogen *Streptococcus agalactiae*. *BMC Genomics* **16**: 419.

Rutherford, K., Parkhill, J., Crook, J., Horsnell, T., Rice, P., Rajandream, M.A., and Barrell, B. (2000) Artemis: sequence visualization and annotation. *Bioinformatics* **16**: 944-945.

Schuchat, A. (1998) Epidemiology of group B streptococcal disease in the United States: Shifting paradigms. *Clin Microbiol Rev* **11**: 497-513.

Seemann, T. (2014) Prokka: rapid prokaryotic genome annotation. *Bioinformatics* **30**: 2068-2069.

Sendi, P., Christensson, B., Uckay, I., Trampuz, A., Achermann, Y., Boggian, K., Svensson, D., Widerstrom, M., and Zimmerli, W. (2011) Group B streptococcus in prosthetic hip and knee joint-associated infections. *J*

Hosp Infect **79**: 64-69.

Sheen, T.R., Jimenez, A., Wang, N.-Y., Banerjee, A., van Sorge, N.M., and Doran, K.S. (2011) Serine-rich repeat proteins and pili promote *Streptococcus agalactiae* colonization of the vaginal tract. *J Bacteriol* **193**: 6834-6842.

Souvorov, A., Agarwala, R., and Lipman, D.J. (2018) SKESA: Strategic k-mer extension for scrupulous assemblies. *Genome Biol* **19**: 153.

Spellerberg, B., Rozdzinski, E., Martin, S., Weber-Heynemann, J., Schnitzler, N., Lütticken, R., and Podbielski, A. (1999) Lmb, a protein with similarities to the LraI adhesin family, mediates attachment of *Streptococcus agalactiae* to human laminin. *Infect Immun* **67**: 871-878.

Sullivan, M.J., Goh, K.G.K., Gosling, D., Katupitiya, L., and Ulett, G.C. (2021) Copper intoxication in group B *Streptococcus* triggers transcriptional activation of the *cop* operon that contributes to enhanced virulence during acute infection. *J Bacteriol*: Jb0031521.

Tande, A.J., and Patel, R. (2014) Prosthetic joint infection. *Clin Microbiol Rev* **27**: 302-345.

Tenenbaum, T., Spellerberg, B., Adam, R., Vogel, M., Kim, K.S., and Schroten, H. (2007) *Streptococcus agalactiae* invasion of human brain microvascular endothelial cells is promoted by the laminin-binding protein Lmb. *Microbes Infect* **9**: 714-720.

Tettelin, H., Masignani, V., Cieslewicz, M.J., Donati, C., Medini, D., Ward, N.L., Angiuoli, S.V., Crabtree, J., Jones, A.L., Durkin, A.S., Deboy, R.T., Davidsen, T.M., Mora, M., Scarselli, M., Margarit y Ros, I., Peterson, J.D., Hauser, C.R., Sundaram, J.P., Nelson, W.C., Madupu, R., Brinkac, L.M., Dodson, R.J., Rosovitz, M.J., Sullivan, S.A., Daugherty, S.C., Haft, D.H., Selengut, J., Gwinn, M.L., Zhou, L., Zafar, N., Khouri, H., Radune, D., Dimitrov, G., Watkins, K., O'Connor, K.J., Smith, S., Utterback, T.R., White, O., Rubens, C.E., Grandi, G., Madoff, L.C., Kasper, D.L., Telford, J.L., Wessels, M.R., Rappuoli, R., and Fraser, C.M. (2005) Genome analysis of multiple pathogenic isolates of *Streptococcus agalactiae*: implications for the microbial "pan-genome". *Proc Natl Acad Sci U S A* **102**: 13950-13955.

Thoendel, M., Jeraldo, P.R., Greenwood-Quaintance, K.E., Yao, J.Z., Chia, N., Hanssen, A.D., Abdel, M.P., and Patel, R. (2016) Comparison of microbial DNA enrichment tools for metagenomic whole genome sequencing. *J Microbiol Methods* **127**: 141-145.

Trampuz, A., Piper, K.E., Jacobson, M.J., Hanssen, A.D., Unni, K.K., Osmon, D.R., Mandrekar, J.N., Cockerill, F.R., Steckelberg, J.M., Greenleaf, J.F., and Patel, R. (2007) Sonication of removed hip and knee prostheses for diagnosis of infection. *N Engl J Med* **357**: 654-663.

Triesenberg, S.N., Clark, N.M., and Kauffman, C.A. (1992) Group B streptococcal prosthetic joint infection following sigmoidoscopy. *Clin Infect Dis* **15**: 374-375.

Wang, Z., Gerstein, M., and Snyder, M. (2009) RNA-Seq: A revolutionary tool for transcriptomics. *Nat Rev Genet* **10**: 57-63.

Whidbey, C., Harrell, M.I., Burnside, K., Ngo, L., Becraft, A.K., Iyer, L.M., Aravind, L., Hitti, J., Adams Waldorf, K.M., and Rajagopal, L. (2013) A hemolytic pigment of Group B Streptococcus allows bacterial penetration of human placenta. *J Exp Med* **210**: 1265-1281.

White, C., Lee, J., Kambe, T., Fritsche, K., and Petris, M.J. (2009) A role for the ATP7A copper-transporting ATPase in macrophage bactericidal activity. *J Biol Chem* **284**: 33949-33956.

Zeller, V., Lavigne, M., Biau, D., Leclerc, P., Ziza, J.M., Mamoudy, P., and Desplaces, N. (2009a) Outcome of group B streptococcal prosthetic hip infections compared to that of other bacterial infections. *Joint Bone Spine* **76**: 491-496.

Zeller, V., Lavigne, M., Leclerc, P., Lhotellier, L., Graff, W., Ziza, J.M., Desplaces, N., and Mamoudy, P. (2009b) Group B streptococcal prosthetic joint infections: a retrospective study of 30 cases. *Presse Med* **38**: 1577-1584.

Zimmerli, W., Trampuz, A., and Ochsner, P.E. (2004) Prosthetic-joint infections. *N Engl J Med* **351**: 1645-1654.

Table 1. Characteristics of six subjects with *Streptococcus agalactiae* periprosthetic joint infection

Subject	Isolate number	Year	Age (years)	Sex	Site of implant	Implant age at revision	Duration of symptoms (days)	*S. agalactiae* isolated from		Preoperative antibiotic treatment	Surgical procedure	Serotype	MLST sequence type	Pilus type	DEG analysis
								Sonicate fluid	Synovial fluid						
1	IDRL-7463	2005	73	Male	Knee	4.5 years	33	□	ND	None	Resection	II	22	2a	Not included
2	IDRL-7656	2006	67	Male	Knee	11.6 years	107	□	ND	Ceftriaxone	Resection	Ia	1651*	1, 2a	Included
3	IDRL-8557	2009	69	Male	Knee	5.4 years	31	□	ND	Cefadroxil, stopped 21 days before revision	Resection	Ia	23	2a	Included
4	IDRL-9433	2012	55	Female	Knee	29 days	69	□	ND	Clindamycin	Poly exchange	V	1	1, 2a	Included
5	IDRL-10197	2015	42	Male	Hip	2 months	44	□	□	None	One-stage exchange	V	1	1, 2a	Not included
6	IDRL-11503	2016	63	Female	Hip	3 months	33	□	□	Levofloxacin	One-stage exchange	V	1	1, 2a	Included

*Novel sequence type

ND, not done

Figure legends

Figure 1. Functional enrichment of outlier *Streptococcus agalactiae* genes in periprosthetic joint infection sonicate fluid compared to NEM316 grown *in vitro*. Genes with $|z| > 3$ were considered outliers. The ratio of enrichment was calculated as the % of genes of a given functional category in the increased or decreased expressed RNA-seq data set/% of genes assigned to the functional category in the *S. agalactiae* genome. Ribosomal protein, rRNA, and tRNA genes were removed. *, significant enrichment amongst genes increased; †, significant enrichment amongst genes decreased in sonicate fluid, with $P < 0.05$ (Fisher's exact test).

Figure 2. (A) Expression levels of genes involved in bacterial adhesion in sonicate fluid of four periprosthetic joint infection (PJI) subjects compared to NEM316 *in vitro*. *, up-regulated outliers in sonicate fluid; †, down-regulated outliers in sonicate fluid.

(B) Expression levels of invasin and immune evasin genes in sonicate fluid of four PJI subjects compared to NEM316 *in vitro*. *, up-regulated outliers in sonicate fluid; †, down-regulated outliers in sonicate fluid.

APPENDIX

Table A1. RNA counts from sonicate fluid of *Streptococcus agalactiae* PJI subjects (*in vivo*).

	No. of predicted genes	No. of protein-coding genes	Total reads counts of quantified transcripts	Read counts of non-rRNA transcripts	% non-rRNA reads	DEG analysis
1	2,031	1,957	56,989	3,483	6.1	Not included
2	2,240	2,166	175,647	88,497	50.4	Included
3	2,062	1,983	324,455	283,023	87.2	Included
4	2,145	2,074	522,023	483,179	92.6	Included
5	2,095	2,020	31,291	1,849	5.9	Not included
6	2,080	2,008	459,667	252,168	54.9	Included

Table A2. RNA counts from *Streptococcus agalactiae* strain NEM316 RNA-Seq (*in vitro*).

	Read counts of non-rRNA transcripts
1	1,530,792
2	1,708,503
3	1,224,999

Table A3. Confidence, coverage, and identity values of predicted nickel transport genes matched to each template in the Phyre2 model

Old locus tag	Gene name	Template PDB code	PDB title	Aligned residues	Alignment Coverage (%)	Confidence (%)	Identity (%)
sag1514	*nikE, cntF*	4FWI	Crystal structure of the nucleotide-binding domain of a dipeptide ABC transporter	1-215	94	100	29
sag1515	*nikD, cntD*	4FWI	Crystal structure of the nucleotide-binding domain of a dipeptide ABC transporter	3-252	95	100	32
sag1516	*nikC, cntC*	4YMU	Crystal structure of an amino acid ABC transporter complex with arginines and ATPs	56-262	76	99.9	13
sag1517	*nikB, cntB*	4YMU	Crystal structure of an amino acid ABC transporter complex with arginines and ATPs	82-309	72	99.9	15
sag1518	*nikA, cntA*	4OER	Crystal structure of NikA from *Brucella suis*, unliganded form	32-533	93	100	41

Figure A1. Phylogenic tree of the cultured isolates and S. agalactiae NEM316 and 2603V/R.

Figure A2. Protein structure homology model of sag1514–1518 **(A-E, respectively)** produced by Phyre2. The predicted protein from sag1514–1518 is shown in blue with the template protein (Table S2: https://doi.org/10.5281/zenodo.5717630) shown in yellow.

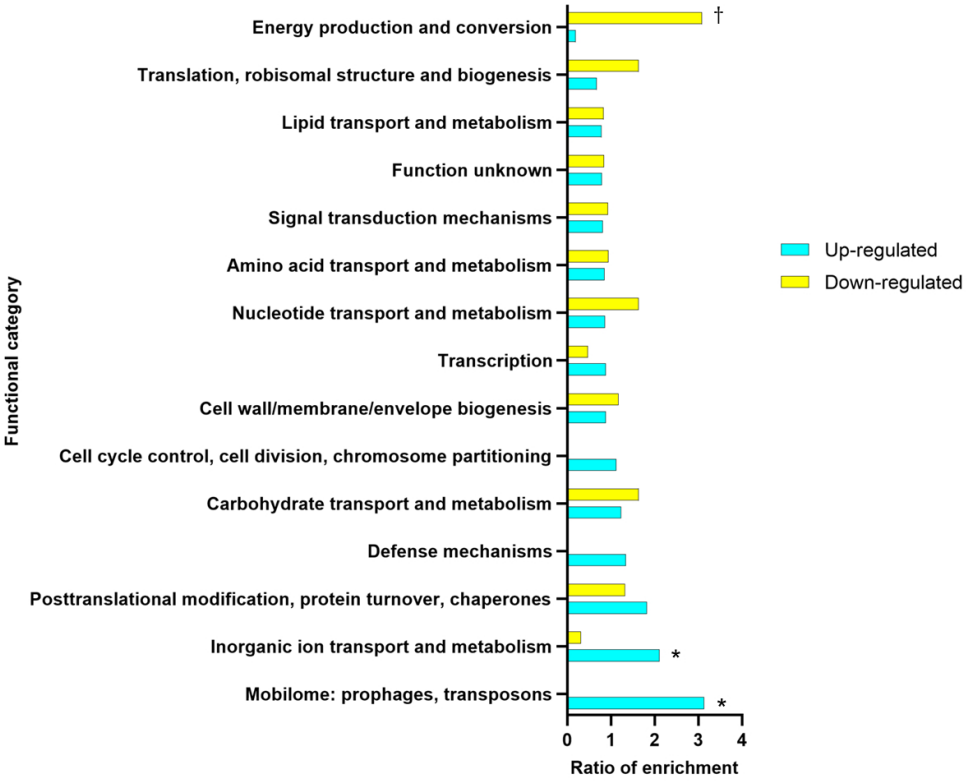

Figure 1

206x170mm (150 x 150 DPI)

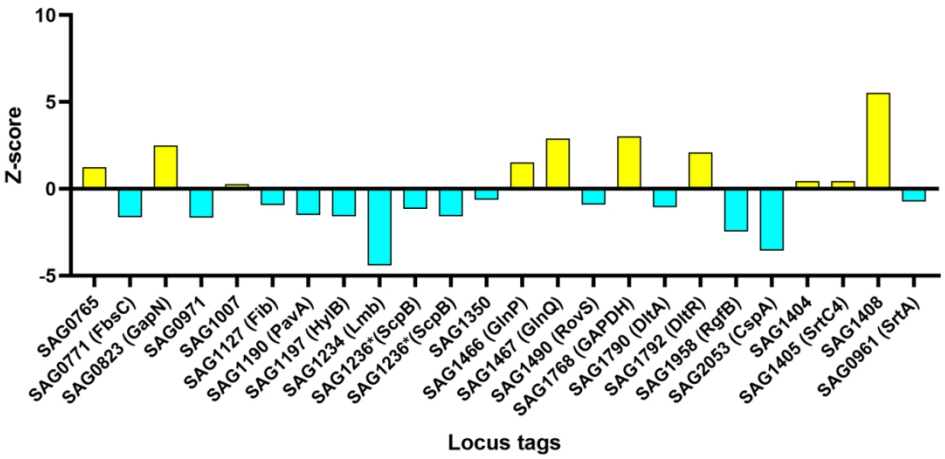

Figure 2A

246x122mm (150 x 150 DPI)

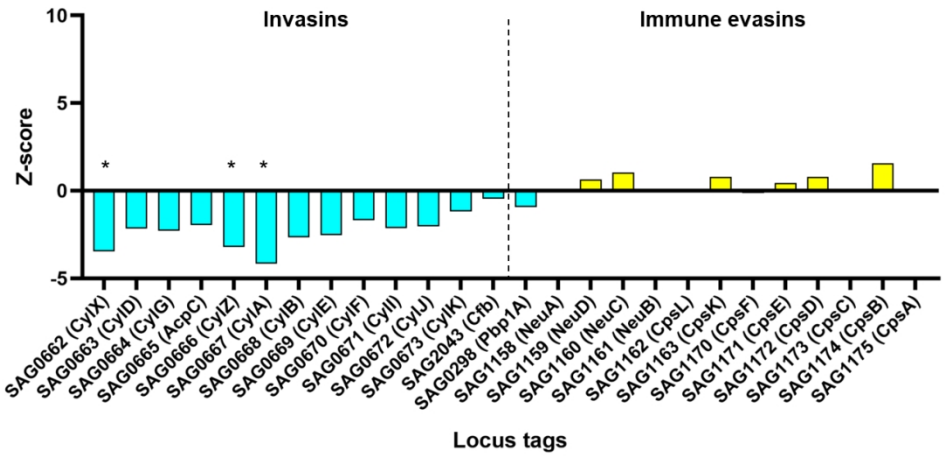

Figure 2B

231x113mm (150 x 150 DPI)

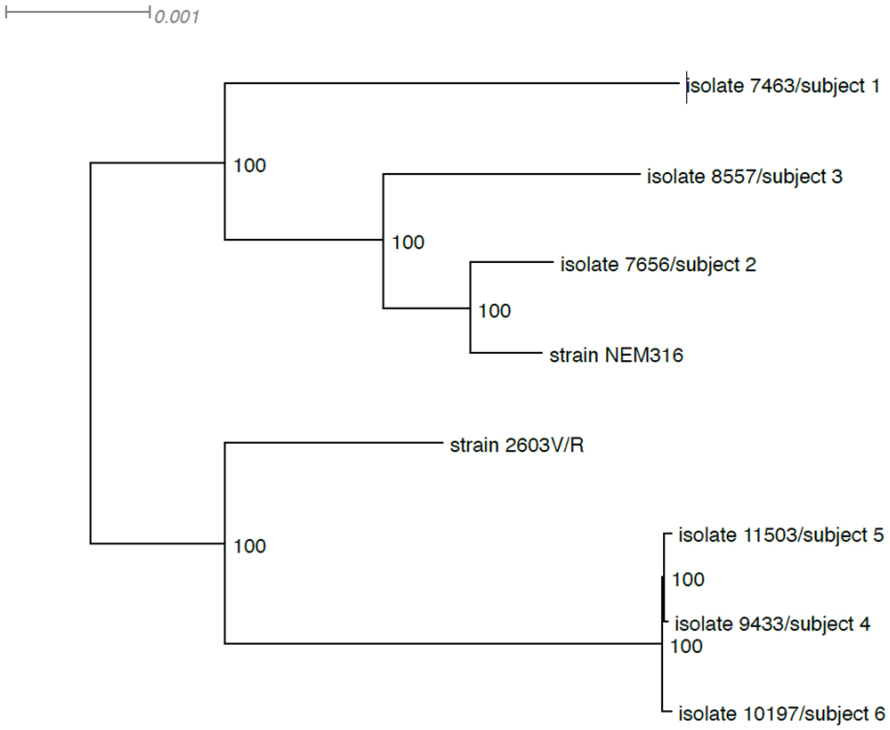

Figure A1

190x145mm (150 x 150 DPI)

Figure A2 (A)

99x112mm (150 x 150 DPI)

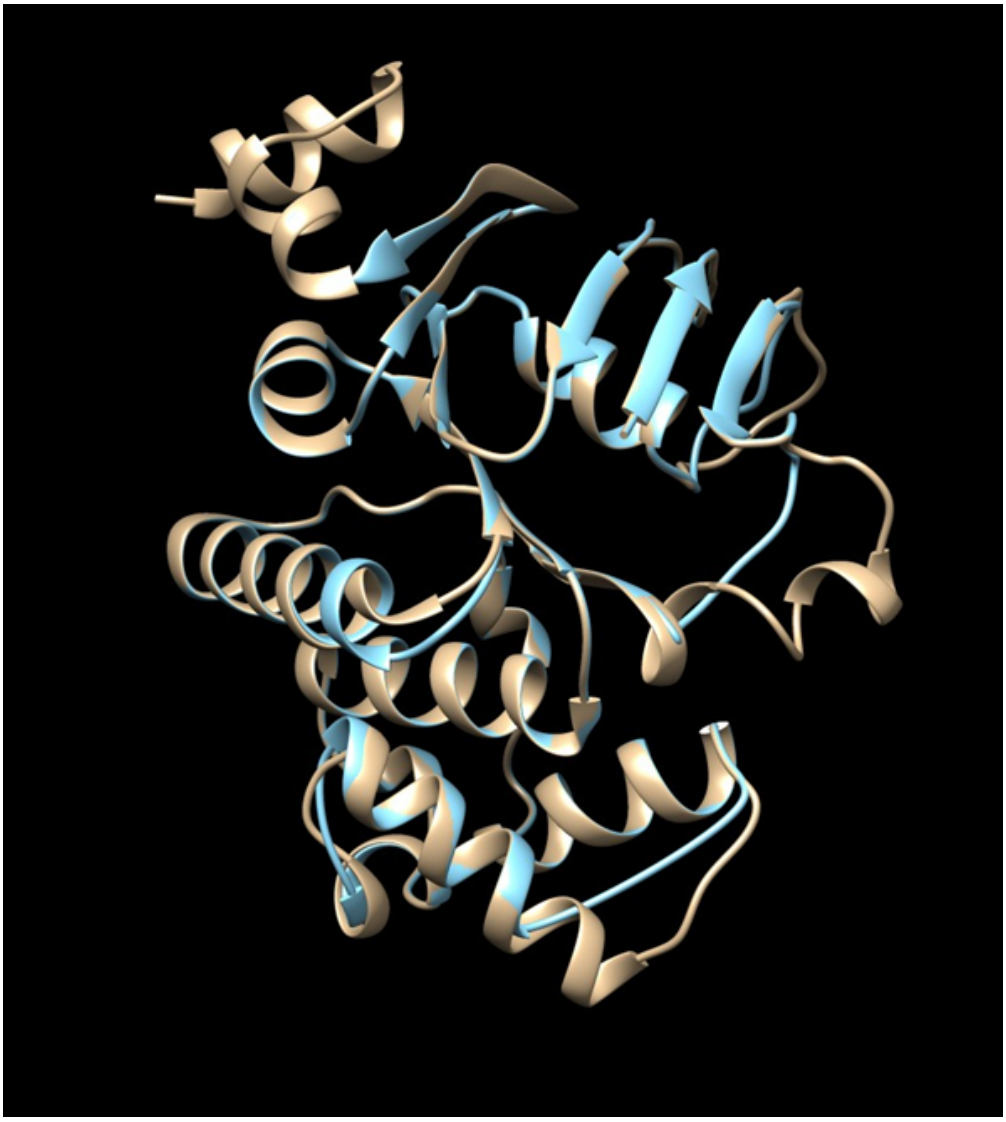

Figure A2 (B)

100x112mm (150 x 150 DPI)

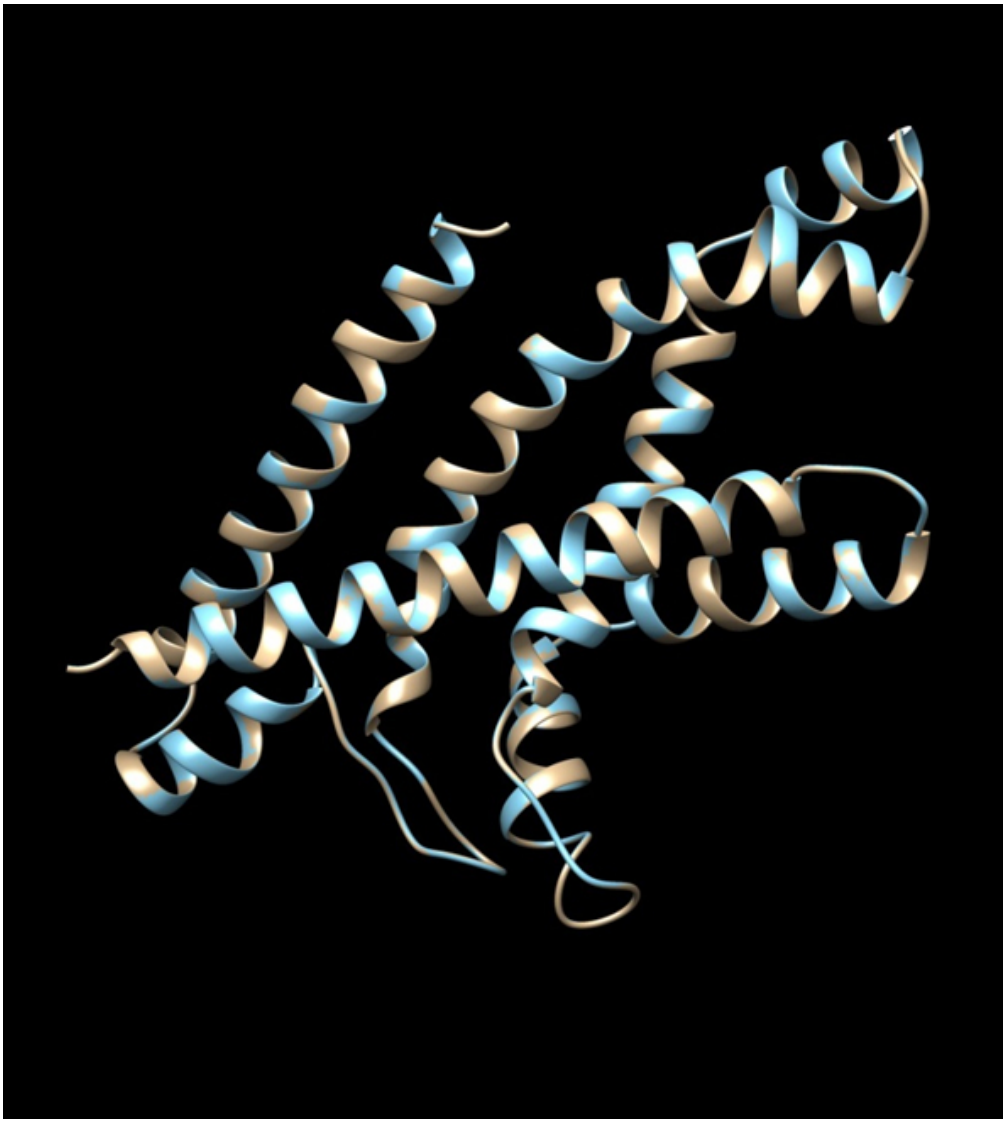

Figure A2 (C)

100x111mm (150 x 150 DPI)

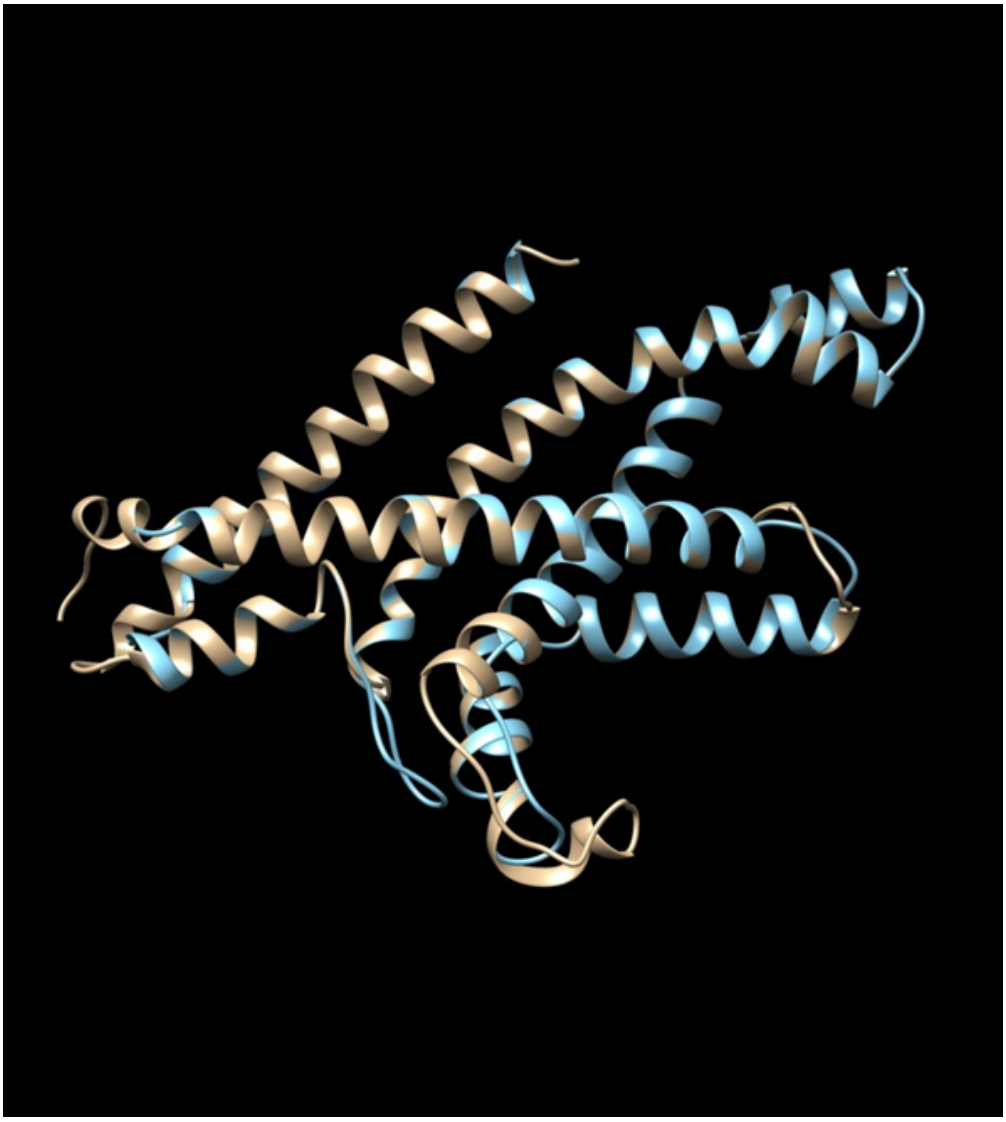

Figure A2 (D)

100x112mm (150 x 150 DPI)

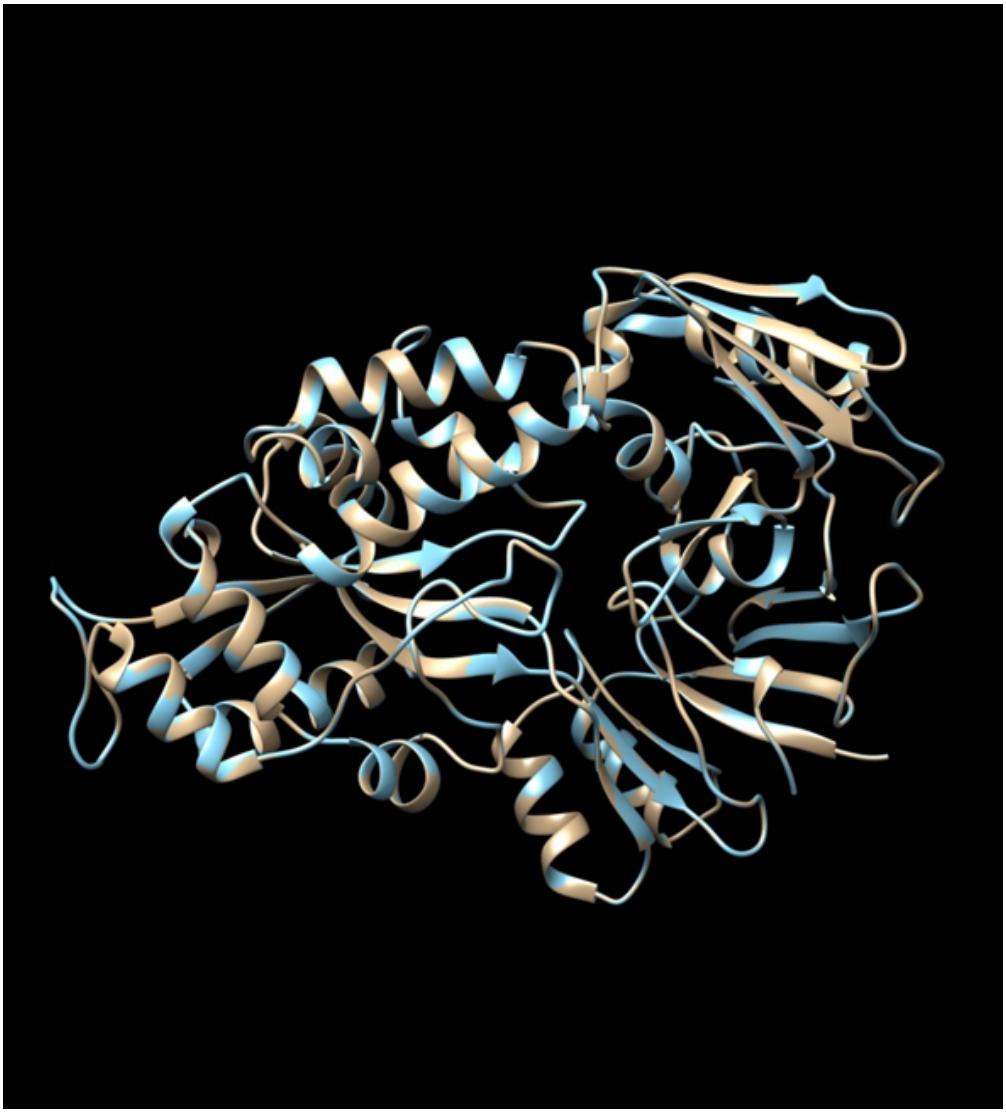

Figure A2 (E)

99x110mm (150 x 150 DPI)

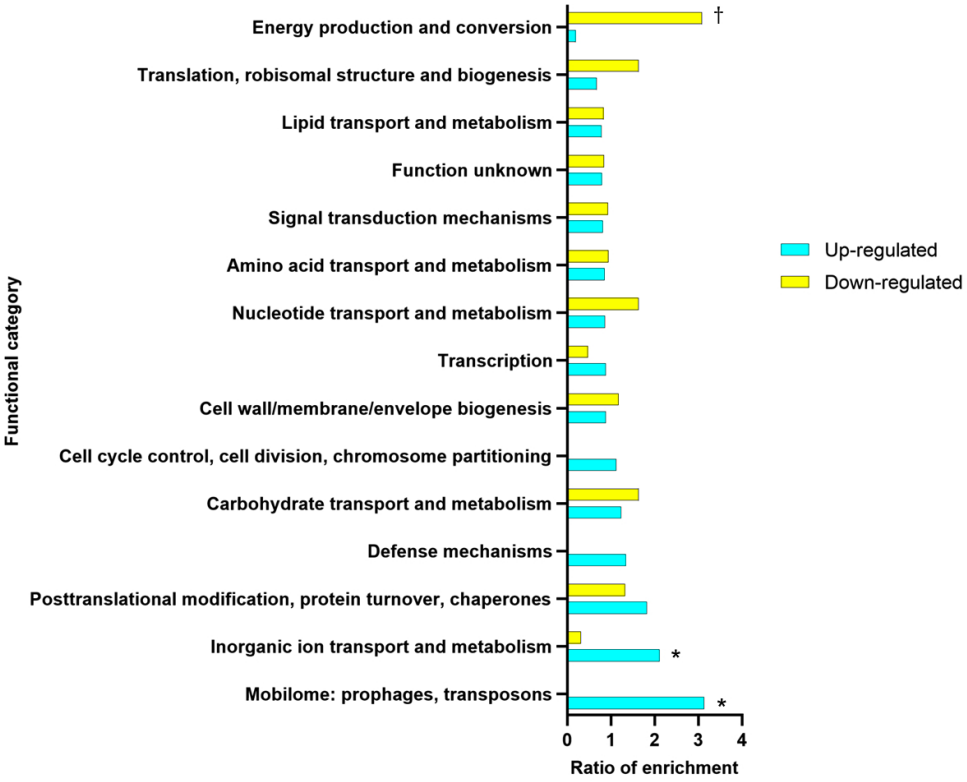

GRAPHICAL ABSTRACT

206x170mm (150 x 150 DPI)